CHAPTER 3

EXPERIMENTAL MODELLING OF MACHINING ENERGY AND CARBON EMISSIONS

This chapter presents the experimental models developed for the measurement of energy consumption and computation of carbon emissions caused during milling process. This chapter also presents a smart metering approach developed for the classification of energy consumption during different operational states.

3.1 INTRODUCTION

The energy characteristics of CNC machine tools are complex and tend to vary with the size & structure of machine tools, and diversity of operational processes. Modern CNC machine tools, based on advanced technology, can perform complex operations with high precision, accuracy, flexibility, and high degree of automation. To perform the required tasks, machine tools are often equipped with complex automated subsystems, which consume high amount of energy. A comprehensive understanding of the dynamic energy behavior of machine tools and their major energy consuming components (spindle motor, axis motors, coolant pump, etc.) is an essential prerequisite for energy efficient machining. Analytical, numerical and experimental modelling techniques have been used in the literature for the energy modelling of machine tools as discussed in chapter 2. Analytical models are based on the fundamental physics of the machining process. In this approach, the basic physical properties of the cutting tool and workpiece materials, along with the kinematics and dynamics of the machining process, are used to predict the machining energy. Analytical models are based on over simplistic assumptions and often involve a large number of complex coefficients. These coefficients are difficult to obtain theoretically, which leads to inaccuracy in the energy prediction. The numerical models

are computer based models, which generally use finite element modelling for prediction of machining performance in terms of cutting force, machining energy, temperature distribution, etc. under different cutting conditions. The performance of numerical models depend on the material model, incorporation of dynamic effects and the capability of the computational system (Kapoor et al., 1998). The major limitations of the numerical models are high computational time, complexity and sensitivity to the material constitutive model, and instability problems with meshing (Kant and Sangwan, 2014). In addition, analytical and numerical models do not capture accurately the various losses in the form of heat, friction, and material deformation, therefore, the actual energy consumption is significantly higher than the theoretically calculated values. Modern machine tools are equipped with a wide range of energy consuming components to accomplish complex machining operations. Their energy characteristics are very diverse which makes it difficult to obtain their energy consumption based on theoretical models. It leads to the need of metering the actual energy demand of the machine tools (Gutowski et al., 2005). Considering the varying energy characteristics of machine tools, experimental models tend to provide an accurate, simple and quick solution for energy consumption modelling. In addition, the energy required for material removal is less than 18% of the total energy consumed by the machine tools. A clear understanding of how and where the energy is consumed during the machining operation is a prerequisite for energy efficient machining (Herrmann et al., 2011). Electrical power data of a machining process is an easily available real time signal, which involves diverse characteristics related to technical specification and operational status of the machine tools. The disaggregation of machining power can provide energy quantification and better transparency in the energy flow of the machining process. This chapter provides a non-intrusive load monitoring approach to obtain the operational state and energy consumption of the machining system using the power data

from the main supply of the machine tool. It reduces the complexity and high cost involved with multi sensor arrangements

Along with high energy consumption, the machining activities are responsible for high carbon emissions. The carbon emissions caused by machining activities are mainly due to energy consumption, coolants, cutting tools, lubricants, raw materials, auxiliary materials, etc. From the literature review, it is observed that the environmental aspects of machining processes have not received the required attention from researchers. In recent years, the industries have become more conscious about the carbon emissions due to strict carbon tax policies, governmental regulations and increasing customer awareness. A few studies have been conducted to analyze the environmental burden of machining activities. Jeswiet and Kara (2008) introduced a new concept of carbon emission signature (CES) to relate the machining energy consumption to the carbon emissions. The CES was calculated based on the energy mix and type of resources used at the power plant. The models for carbon emissions caused by various factors during machining process have been discussed by some researchers (Li et al., 2015; Narita and Fujimoto, 2009; Zhang et al., 2017). Quantification of energy consumption and carbon emissions for a machining process is the first step towards improving the energy and carbon emission performance of the machining processes. This chapter provides experimental models to calculate the energy consumption and carbon emissions for a machining process.

This chapter is divided into two parts. In the first part, models for energy consumption by different components of the machine tool is developed. A structured algorithm is developed for identification of the operational state of the machine tool. In the second part, the experimental models for the carbon emissions caused during the machining process are provided.

3.2 EXPERIMENTAL SET UP

The details of the experimental set up including the machine tool, power measurement system and workpiece material are provided in this section.

3.2.1 Machine Tool

In the current study, the energy characteristics of different machine tool components were experimentally investigated for a 3-axis CNC vertical milling center (LMW klein KODI 40). The machine tool is manufactured in India. The technical specifications of the VMC (LMW klein KODI 40) machine tool are provided in Table 3.1. The term 'machine tool' refers to VMC (LMW klein KODI 40) machine tool in the rest of the chapter.

Table 3.1 Technical specifications of the LMW klein KODI 40 VMC

CNC Vertical milling center		
Make	LMW klein KODI 40	Unit
Power supply	3 Phase AC 415 V, 50 Hz	-
CNC system	Fanuc 0i-MB	-
Positioning accuracy (X, Y, and Z-axis)	0.02	Mm
Repeatability	±0.003	Mm
Machine size (L × B × H)	3230 × 1500 × 3045	Mm
Floor space required (approx.)	5	m^2
Machine weight (approx.)	3500	Kg
Air requirement at NTP	100	Lpm
Table travel (X × Y × Z)	(500 × 410 × 460)	Mm
Table size	750 × 430	Mm
Maximum weight on table	300	Kg
Spindle speed range	150 – 8000	RPM
Spindle motor power (Cont./30min)	5.5/7.5	kW
Spindle motor maximum torque (Cont./30min)	35/47.7	Nm
Maximum spindle temperature above ambient	15	°C
ATC capacity (number of tools)	20	-
Feed motor power (X and Y)	1.6	kW
Feed motor power (Z)	3	kW
Coolant pump motor	1.1	kW
Coolant tank capacity	300	Liters

The total electrical power consumption of the machine tool was measured at the main power supply of the electrical cabinet of the machine tool. Three MECO M1 current transducers were used to measure the three phase input current of the machine tool. The voltage and current signals were acquired and sampled using NI-9244 and NI-9227 data acquisition cards, respectively. NI cDAQ-9178 compact data acquisition USB chassis was used to process the data at single interface. The recorded power and energy data was visualized and stored using the LabVIEW programming interface. The data sampling frequency was kept at 10Hz. The schematic and actual experimental set-up are shown in Figures 3.1 and 3.2, respectively.

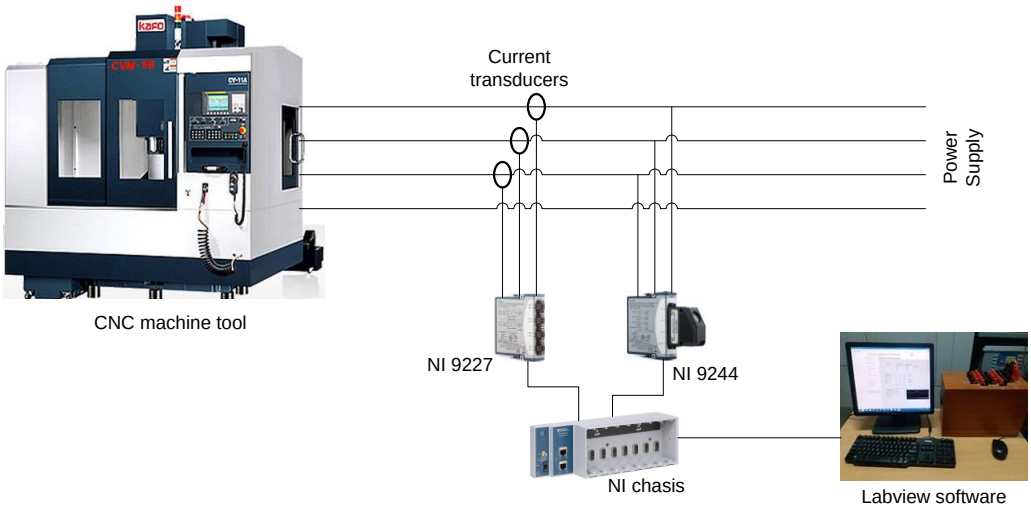

Figure 3.1 The schematic diagram of the experimental set-up used for power data acquisition

3.2.2 Workpiece and Cutting Tool Material

The sample material used for this research is 6351-T6 aluminum alloy. This material is widely used in different industries such as construction, automotive, and transportation, due to its light weight, high corrosion resistance, ductility, conductivity, and yield resistance. According to a study conducted by Pusavec et al. (2010) for the sustainability assessment of different materials, aluminum has the best sustainability performance as compared to stainless steel, steel, titanium, cast iron, and copper alloys.

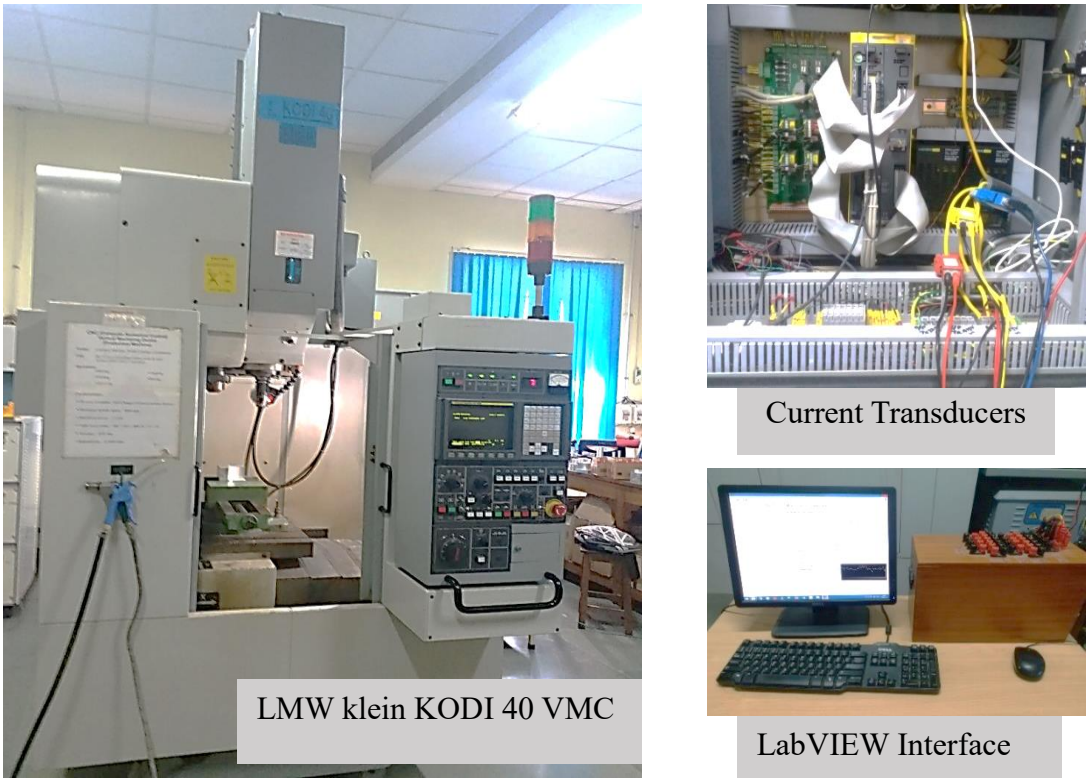

Figure 3.2 The actual experimental set-up used for power data acquisition

In their study, the sustainability of the materials was assessed based on the availability of the material, recycling potential, pollution during machining, life of the material, and cost of the final product. The mechanical properties and chemical composition of the workpiece material are given in Tables 3.2 and 3.3. The cutting tool used for experimentation in this research work was high speed steel solid end mill with four flutes.

Table 3.2 Mechanical properties of the workpiece material

Property	**Value**	**Unit**
Density	2.71	g/cm^3
Brinell Hardness	95	–
Vickers hardness	107	–
Ultimate tensile strength	310	MPa
Yield tensile strength	283	MPa
Specific heat capacity	0.890	J/g – °C
Thermal conductivity	176	W/m – K

Table 3.3 Chemical composition of the workpiece material

Aluminum	Copper	Iron	Magnesium	Manganese	Silicon	Titanium	Zinc
95.9 – 98.5 %	≤ 0.1%	≤ 0.5%	0.4 – 0.8 %	0.4 – 0.8 %	0.7 – 1.3 %	≤ 0.2%	≤ 0.2%

3.2.3 Surface Roughness Measurement

The surface roughness of the finished samples was measured using Taylor Hobson Talysurf. The technical specifications of the Talysurf are given in Table 3.4.

Table 3.4 Technical specifications of the surface roughness measurement instrument

Factor	Specification
Make	Taylor Hobson
Model	Form Talysurf Intra
Speed of traverse	1 mm/sec – 10 mm/sec
Nominal measuring range	1 mm
Resolution	16 nm
Pickup	Inductive type
Measurable parameters	R_a/ R_z/ R_t

3.3 MODELLING OF MACHINING ENERGY CONSUMPTION

The important energy consuming components for machine tools and their energy consumption were discussed in Chapter 2. In this section, the energy consumption models developed for start-up, basic module, spindle motor, feed motors, automatic tool changer, coolant pump, lubrication pump, material removal, and losses are discussed for LMW klein KODI 40 VMC.

3.3.1 Start-up Energy ($E_{start-up}$)

The machine tool experiences a power spike during the start-up period. The instant rise in the power demand causes additional energy consumption. The power profile for the start-up phase of the machine tool was measured experimentally and shown in Figure 3.3.

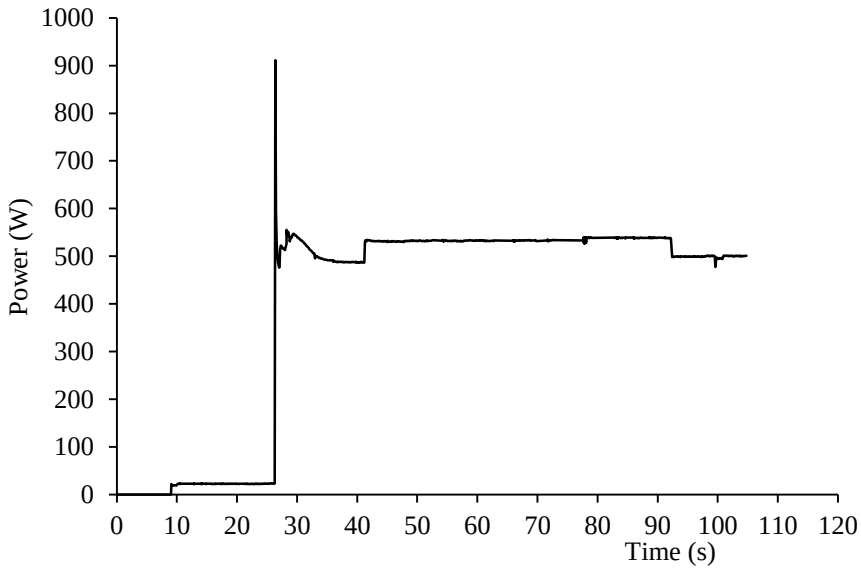

Figure 3.3 Start-up power profile for LMW klein KODI 40 VMC

3.3.2 Stand-by Energy ($E_{stand-by}$)

Stand-by energy is the energy consumed when the machine tool is in stand-by mode, i.e. machine tool is switched on, the auxiliary components are ready but not operational, spindle and feed movements are absent, and cutting operation has not started. It is an intrinsic characteristic of a machine tool. The stand-by power depends on the machine tool design and its modules like fan motor, controller, servo system, light, relays, etc. The stand-by power of a machine tool is generally constant with a little fluctuation due to current and voltage instability and therefore the average value is calculated. In the present study, the stand-by power was measured experimentally for ten seconds and the average was calculated as follows:

$$P_{stand-by} = \frac{\sum_{i=1}^{N} P_{stand-by,i}}{N} \tag{3.1}$$

where $P_{stand-by,i}$ is the measured stand-by power value at measurement point *i* and N is the number of measurement points. The stand-by energy was calculated as follows:

$$E_{stand-by} = P_{stand-by} * t_{stand-by} \tag{3.2}$$

where $t_{stand-by,i}$ is the stand-by time. In the present study the average stand-by power for LMW KODI40 VMC was found to be 500W.

3.3.3 Unloaded Spindle Energy (E_{u-SR})

The spindle system of a machine tool consists of spindle motor, motor drive and mechanical transmission system. The machine tool spindle delivers the required mechanical power, cutting speed and torque required for cutting operation. Unloaded spindle power is the power consumed by the spindle system in a stable state when it is operating at a constant speed at no load condition. In the present study, the power consumption by FANUC alpha 6i servo motor was analyzed, which is used for spindle rotation in the machine tool. The technical specifications of the FANUC alpha 6i servo motor are given in Table 3.5. The spindle speed–output curve for the FANUC alpha 6i servo motor is shown in Figure 3.4. The power and torque curves for different motors may vary based on the motor design. For the machine tool under investigation, it varies as constant torque followed by constant power.

Table 3.5 Technical specifications of the spindle motor for LMW klein KODI 40 VMC

Motor	**FANUC alpha 6i servo motor**
Speed range	150-8000 RPM
Motor power (Cont./3min)	5.5/7.5 kW
Maximum Torque	35/47.7 Nm

Figure 3.4 shows the nominal power available at maximum loading conditions and it reflects the maximum capacity of the motor. The actual unloaded spindle power is less than the nominal power.

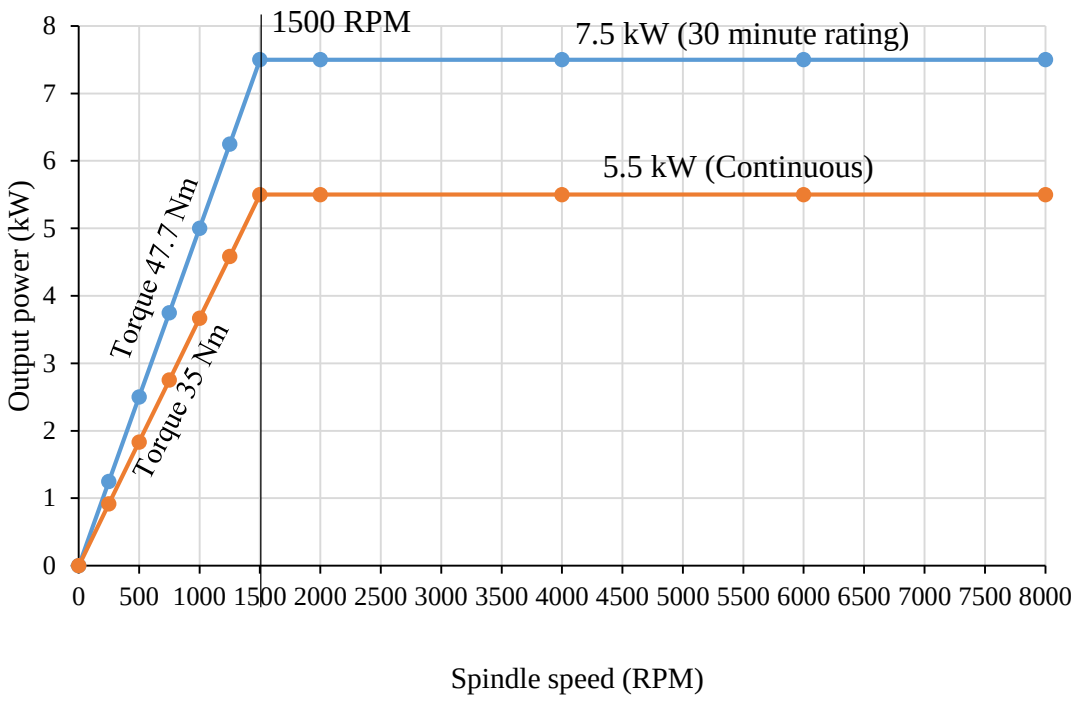

Figure 3.4 FANUC alpha 6i spindle motor power curve

The unloaded spindle power and torque vary with the rotational speed of the motor and therefore can be mathematically modelled as a function of spindle RPM. In the present study, an experimental model was established for the unloaded spindle power consumption (P_{u-SR}) with rotational speed using Minitab 17 software. P_{u-SR} was measured at different rotational speeds ranging from 150-8000 RPM. The spindle was activated five times at each RPM and the average of five values was calculated to obtain the P_{u-SR} at the respective RPM. The average power consumption of unloaded spindle rotation at different rotational speeds is given in Table 3.6.

Table 3.6 Unloaded spindle rotation power at different rotation speeds

n (RPM)	150	1000	2000	3000	4000	5000	6000	7000	8000
P_{u-SR} **(kW)**	0.05	0.178	0.335	0.452	0.576	0.708	0.799	0.895	1.024

Regression analysis was carried out to obtain a mathematical model between unloaded spindle power and rotation speed, using Minitab 17 software. It was observed that the

unloaded spindle power varied linearly with the rotational speed and a linear model was obtained, as follows:

$$P_{u-SR} = 68.86 + 0.1216n \quad (3.3)$$

The model was tested for model fitness and adequacy as shown in Figure 3.5.

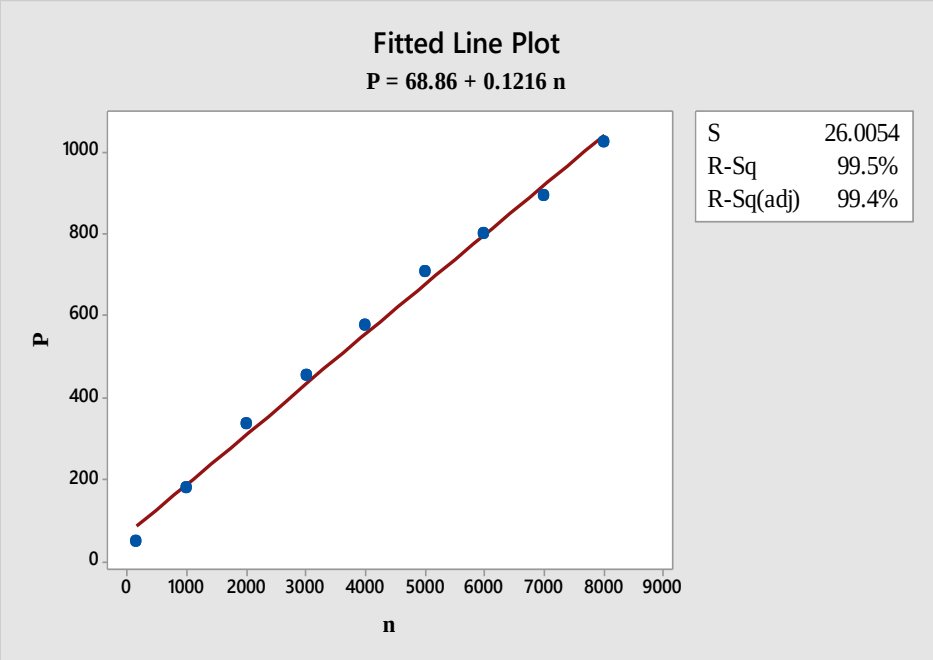

Figure 3.5 Model fitness for unloaded spindle power

The coefficient of determination (R^2), is widely used as a measure of the degree of fitness for the predictive models. It is defined as the ratio of explained variation to the total variance in the model. The value of R^2 obtained was 99.5% which represents that 99.5% of the total variance can be explained by the mathematical model. The adjusted R^2 was 99.4%. It indicates that 99.4% of the total variance can be explained by the proposed mathematical model on the consideration of the significant factors.

3.3.4 Feed Motion Energy (E_{feed})

The feed system of a machine tool consists of the feed motors and feed transmission system. The feed power comprises of the power consumed by the feed servo motors and

the mechanical transmission losses in the system. It is the power required to position the machine tool table and cutting tool at the precise location based on the specific speed and direction of movement. The feed motion can be in horizontal as well as vertical directions.

For horizontal movements, the feed power depends on the cutting and friction torques. However, in case of vertical feed, the gravitational force is also applicable as an additional load. This results into different power consumption for upward and downward feed motions.

The present study provides a simplified experimental modelling approach to calculate the power required for movement of machine tool axes. The power consumed by the feed system depends on the axis feed and can be mathematically expressed in terms of feed. The feed motion power for each of the three axes at different feed speeds and directions were measured. In the present study, the power consumption by FANUC alpha 8i and 12i servo motors were analyzed, which are used as feed axis motors in LMW klein KODI 40 VMC. The technical specifications of the feed system for the machine tool are given in Table 3.7. The X- and Y- axis motors are same and their power characteristics were observed to be similar in both directions. The average power consumption of unloaded X- and Y- feed axis motors at different feed rates is given in Table 3.8.

Table 3.7 Technical specifications of the feed system for LMW klein KODI 40 VMC

Rapid feed rate (X-,Y- and Z-axis)	24, 24 and 20 m/min
Cutting feed rate	1-10000 mm/min
Jog feed rate	0-1260 mm/min
Feed motor power (X- and Y-axis)	1.6 kW (Fanuc α8i)
Feed motor power (Z-axis)	3.0 kW (Fanuc α12i)
Feed motor torque (X- and Y-axis)	8.0 Nm
Feed motor torque (Z-axis)	12.0 Nm

Table 3.8 Unloaded X- and Y- axis feed motor power at different feed rates

Feed (mm/min)	$P_{feed-x,y}$ (W)	Feed (mm/min)	$P_{feed-x,y}$ (W)
50	17	5000	122
100	18	5500	136
500	22	6000	150
1000	29	6500	159
1500	42	7000	171
2000	51	7500	182
2500	64	8000	197
3000	71	8500	212
3500	83	9000	225
4000	100	9500	238
4500	111	10000	250

Using regression analysis, it was found that unloaded X- and Y- axis feed motor power and feed rate follows a linear model as shown in Figure 3.6 and given as:

$$P_{feed-x,y} = 6.552 + 0.02383 * \mathrm{f} \tag{3.4}$$

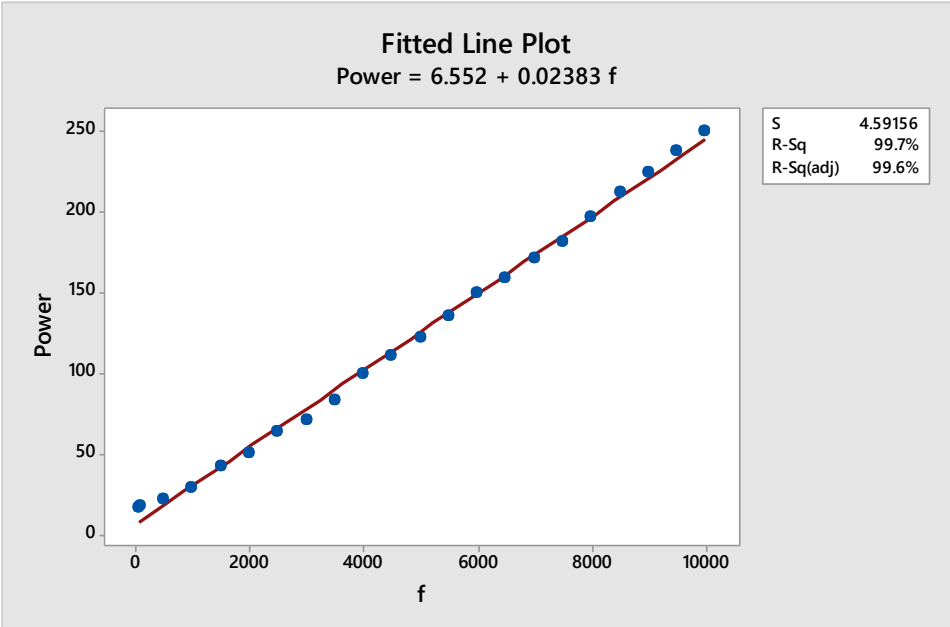

Figure 3.6 Model fitness for unloaded X- and Y- axis feed motor

The linear mathematical model was tested for model fitness and adequacy. The value of R^2 was 99.7%, which represents that 99.7% of the total variance can be explained by

the mathematical model. The value of coefficient R^2 (adj) was 99.6%. It indicates that the proposed mathematical model can explain 99.6% of the total variance on the consideration of the significant factors. The average power consumption of unloaded Z-axis feed motor for upward movement and downward movements at different feed rates is given in Tables 3.9 and 3.10.

Table 3.9 Unloaded Z- axis feed motor power for upward direction at different feed rates

Feed (mm/min)	$P_{feed-z+}$ **(W)**	**Feed (mm/min)**	$P_{feed-z+}$ **(W)**
50	12	5000	521
100	14	5500	574
500	48	6000	623
1000	97	6500	669
1500	147	7000	727
2000	198	7500	779
2500	251	8000	835
3000	301	8500	884
3500	369	9000	934
4000	421	9500	986
4500	469	10000	1041

Table 3.10 Unloaded Z- axis feed motor power for downward direction at different feed rates

Feed (mm/min)	$P_{feed-z-}$ **(W)**	**Feed (mm/min)**	$P_{feed-z-}$ **(W)**
50	-4	5000	-216*
100	-6	5500	-225*
500	-23	6000	-240*
1000	-39	6500	-250*
1500	-59	7000	-278*
2000	-77	7500	-279*
2500	-124	8000	-311*
3000	-136	8500	-313*
3500	-162	9000	-328*
4000	-179	9500	-366*
4500	-199	10000	-405*

* Negative value indicates that the power is below the basic power consumption

Using regression analysis, it was found that average power consumption of unloaded Z-axis feed motor and feed rate follow linear models as follows:

$$P_{feed-z+} = -2.994 + 0.01043 * \mathrm{f} \quad \text{(upward movement)} \tag{3.5}$$

$$P_{feed-z-} = -12.24 - 0.03756 * \mathrm{f} \quad \text{(downward movement)} \tag{3.6}$$

The mathematical models were tested for model fitness and adequacy as shown in Figures 3.7 and 3.8. The results show that the linear models are able to explain the variance with high accuracy.

The total feed power can be calculated as the summation of the feed powers in X, Y and Z-directions as follows:

$$P_{feed} = P_{feed-x,f_x} + P_{feed-y,f_y} + P_{feed-z,f_z} \tag{3.7}$$

where P_{feed} is the feed power at the cutting feed, P_{feed-x,f_x} is the power consumed by x-axis motor at speed of f_x, P_{feed-y,f_y} is the power consumed by y-axis motor at speed of f_y, P_{feed-z,f_z} is the power consumed by z-axis motor at speed of f_z.

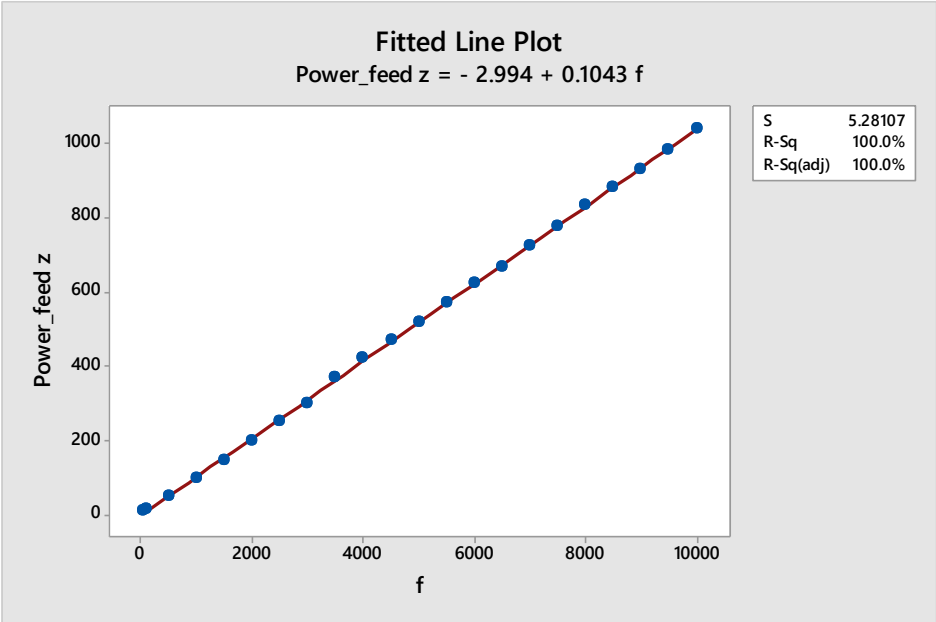

Figure 3.7 Model fitness for Z-axis motor power (upward movement)

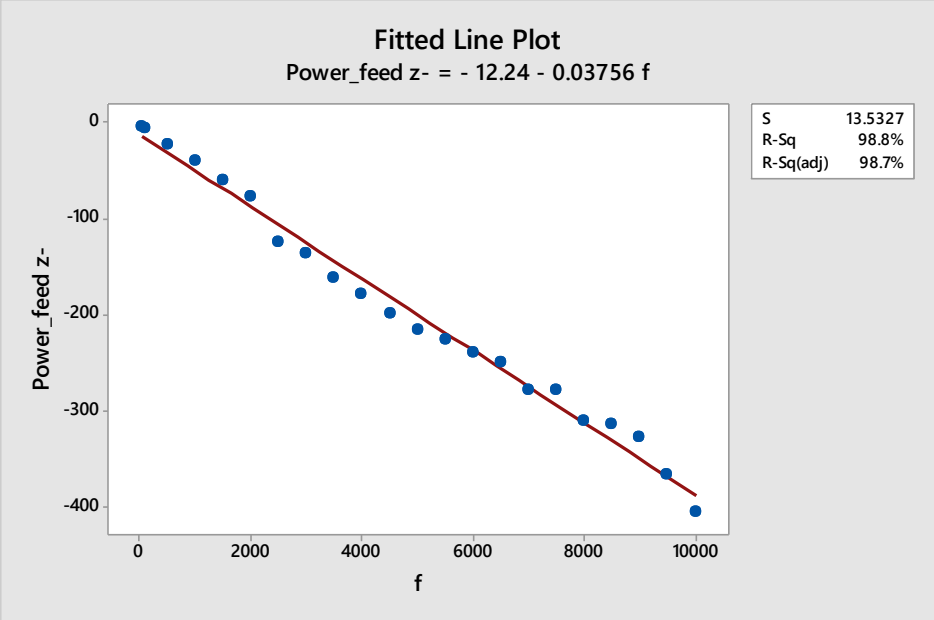

Figure 3.8 Model fitness for Z-axis motor power (downward movement)

The cutting feed can be calculated as the root mean square if the axes are moving simultaneously:

$$f = \sqrt{f_x^2 + f_y^2 + f_z^2} \tag{3.8}$$

The rapid feed power can be calculated similarly as:

$$P_{feed}^r = P_{feed-x}^r + P_{feed-y}^r + P_{feed-z}^r \tag{3.9}$$

where P_{feed}^r is the total feed power for the rapid motion; P_{feed-x}^r, P_{feed-y}^r and P_{feed-z}^r are the power consumed by the X-, Y-, and Z-axis motors respectively for rapid feed motion. The rapid feed powers for the three axis are given in Table 3.11. The energy required to facilitate the feed motion can be obtained by multiplying the feed power with the activation time of each feed motor.

Table 3.11 Rapid feed power for X-, Y- and Z-axis feed motors for LMW klein KODI 40 VMC

Axis	**Feed (mm/min)**	**Power (kW)**
X- and Y-axis	12000	0.36
Z-axis, upward movement	12000	1.14
Z-axis, downward movement	9000	-0.32*

* Negative value indicates that the power is below the basic power consumption

3.3.5 Auxiliary Components Energy

Auxiliary components include coolant pump, ATC, lubricant system, etc. The power consumption of the auxiliary components is generally constant and can be obtained from technical specification manual of the machine tool or measured experimentally.

3.3.5.1 Automatic tool change energy (E_{ATC})

E_{ATC} is the energy required by the automatic tool changing system for changing the cutting tools. It comprises the energy required for rotation of tool magazine to the specific post based on NC program, loading and unloading of the cutting tools, and arm movement. The energy consumption by the automatic tool changing system can be modelled as follows:

$$E_{ATC} = P_{ATC} * t_{ATC} * n_{tool} \tag{3.10}$$

where P_{ATC} is the power demand of the ATC motor, t_{ATC} is the activation time of ATC motor and n_{tool} is the number of tool changes. The number of tool changes can be computed based on the cutting time and the tool life. t_{ATC} is calculated as follows:

$$t_{ATC} = \frac{position_{initial} - position_{assigned}}{num_{post} * n_{magazine}} \tag{3.11}$$

where $position_{initial}$ is the initial magazine position, $position_{assigned}$ is the position of the tool magazine assigned by the NC program, num_{post} is the number of tool posts in the magazine, and $n_{magazine}$ is the rotational speed of the tool magazine.

The P_{ATC} is constant for a specific machine tool. For LMW klein KODI 40 VMC, the P_{ATC} was experimentally measured to be 0.25 kW. The other specifications of the ATC system are given in Table 3.12.

Table 3.12 ATC specifications for LMW klein KODI 40 VMC

Tool shank	MAS BT 40
Number of tool post	20
Tool change time- tool to tool	2.5 sec
Tool change time- chip to chip	6.5 sec

3.3.5.2 Coolant pump energy ($E_{coolant}$)

Coolant pump supplies the cutting fluid to the cutting area. The cutting fluid helps to dissipate the heat, reduce friction in the cutting zone, and flush away the chips. $E_{coolant}$ is the energy required by the coolant pump to supply the coolant in the cutting area. It is calculated as follows:

$$E_{coolant} = P_{coolant} * t_{coolant} \tag{3.12}$$

where $P_{coolant}$ is the coolant motor power and $t_{coolant}$ is the activation time of the coolant motor. The coolant motor power is also constant for a specific machine tool and can be obtained from machine tool technical manual or measured experimentally. $P_{coolant}$ of LMW klein KODI 40 VMC is 1.1 kW. The power profile of coolant pump is shown in Figure 3.9.

3.3.5.3 Lubrication pump energy ($E_{lubricant}$)

Lubricating oils are important for prevention of wear and corrosion of the machine tool slideways and bearings. $E_{lubricant}$ is the energy required by the lubrication pump to supply the lubricating oil to the machine tool. It is calculated as follows:

$$E_{lubricant} = P_{lubricant} * t_{lubricant} \tag{3.13}$$

where $P_{lubricant}$ is the lubrication pump power and $t_{lubricant}$ is the activation time of the lubrication pump. A slideway lubrication pump, also known as cycle pump, is used in the machine tool to supply lubricant oil to X-, Y-, Z- axis slideways and ballscrews at 30

minutes interval. The unit is designed to run intermittently and is best suited for single shot centralized system. $P_{Lubricant}$ of LMW klein KODI 40 VMC was measured experimentally as 0.28 kW. The Lubrication pump power profile is shown in Figure 3.10.

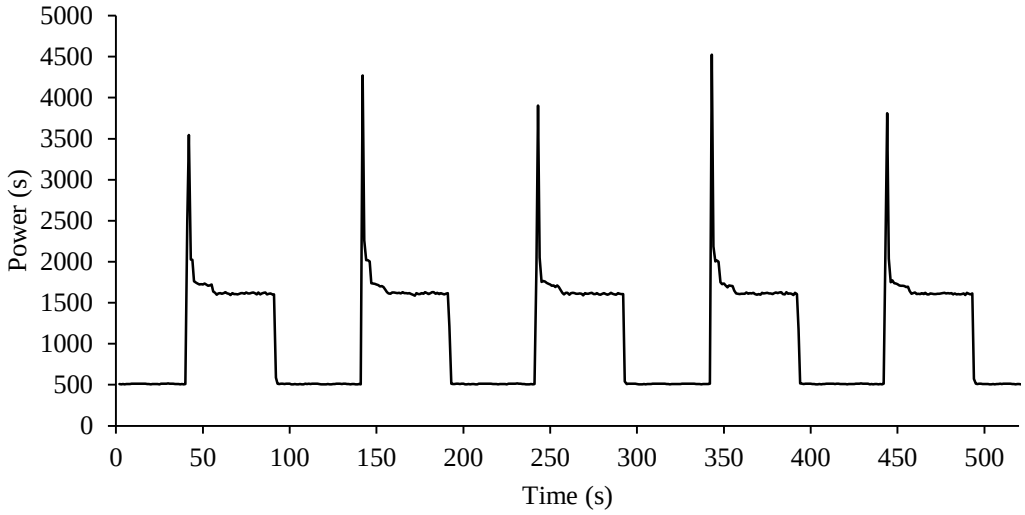

Figure 3.9 Coolant pump power profile for LMW klein KODI 40 VMC

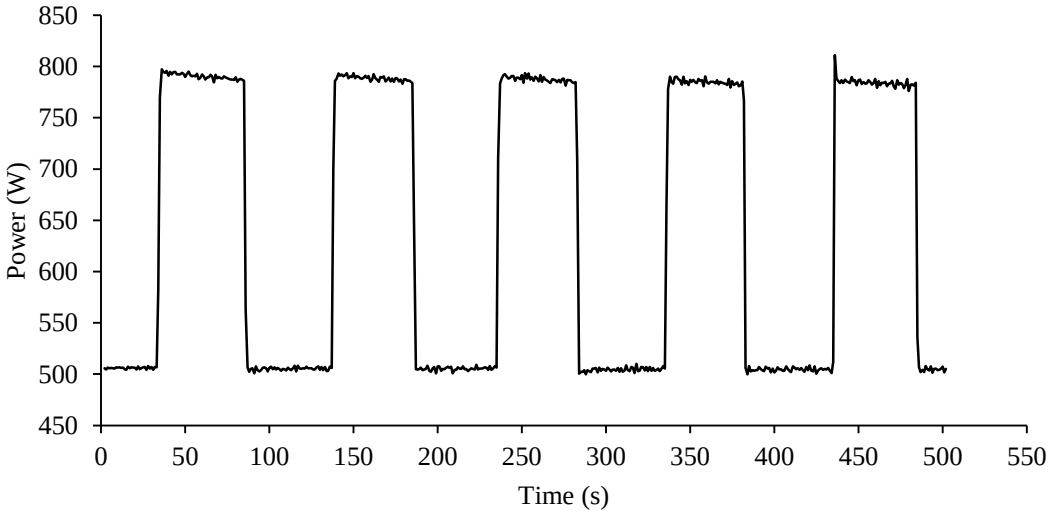

Figure 3.10 Lubrication pump power profile for LMW klein KODI 40 VMC

3.3.6 Material Removal Energy ($E_{cutting}$)

Material removal energy or cutting energy is the energy required to remove the material from the workpiece in the form of chips. Material removal energy can be calculated as the product of cutting power ($P_{cutting}$) and cutting time ($t_{cutting}$).

$$E_{cutting} = P_{cutting} * t_{cutting} \tag{3.14}$$

The cutting power can be calculated in different ways. The various models for cutting power prediction are discussed in chapter 2. The cutting power is commonly calculated as the product of cutting force ($F_{cutting}$) and cutting speed (v).

$$P_{cutting} = F_{cutting} * v \tag{3.15}$$

The cutting force can be measured experimentally or modelled theoretically. The cutting power can also be estimated based on the specific cutting energy (k) as

$$P_{cutting} = k * MRR \tag{3.16}$$

The specific cutting energy is the energy required for removal of unit volume of workpiece material in the form of chips. It is a property of the workpiece material and reflects its machinability. However, the theoretical models of cutting force or specific cutting energy involve a number of coefficients, which are difficult to obtain. Measurement of cutting force is also complex as it involves dynamometer set up. In this study, the cutting power was experimentally obtained as discussed in section 3.3.7.

The cutting time is calculated based on the machining parameters and tool path. For face milling process, it can be calculated as follows (Li et al., 2017):

$$t_{cutting\_mill} = \frac{L+d_a}{n\, f_z\, z} \tag{3.17}$$

where L is the length of the workpiece (mm), n is the spindle speed (RPM), f_z is the feed rate (mm/tooth), z is the number of inserts, and d_a is the approach distance (mm). The approach distance is calculated as follows:

$$d_a = \frac{D}{2} - \sqrt{\left(\frac{D}{2}\right)^2 - \left(\frac{a_e}{2}\right)^2} \tag{3.18}$$

where D is the diameter of the cutting tool (mm) and a_e is the width of cut (mm). The cutting time for turning process can be calculated as follows:

$$t_{cutting\_turn} = \frac{60l}{fn} = \frac{60\pi Dl}{fv} \tag{3.19}$$

where l is the cutting length (mm), f is the feed rate (mm/rev), D is the diameter of the workpiece (mm), and v is the cutting speed (mm/min).

3.3.7 Additional Energy Losses (E_{add})

The spindle motor, feed motors and transmission system are subjected to additional mechanical and electrical losses on the application of cutting load. The additional energy losses occur due to the above mentioned losses in the system. It is calculated as the product of additional power loss (P_{add}) and cutting time.

$$E_{add} = P_{add} * t_{cutting} \tag{3.20}$$

The additional power loss can be modelled as a quadratic function of cutting power (Hu et al., 2010).

$$P_{add} = a_0 P_{cutting} + a_1 P_{cutting}^2 \tag{3.21}$$

where a_0 and a_1 are the additional load loss coefficients. In the present study the cutting power and additional power loss were collectively obtained based on experimental measurements. The total power demand for the machining operation was measured experimentally. The power required for basic operation, unloaded spindle system, spindle acceleration, feed system, and auxiliary components was subtracted from the total power to obtain the cutting power and additional power loss collectively.

$$P_{cutting} + P_{add} = P_{in} - P_{stand-by} - P_{u-SR} - P_{sp-acc} - P_{feed} - P_{ATC} - P_{coolant} - P_{lubricant} \quad (3.22)$$

3.4 DEVELOPMENT OF A SMART METERING APPROACH FOR MACHINE TOOLS

Measurement and monitoring of energy is the first step towards energy efficient manufacturing. Herrmann et al. (Herrmann et al., 2011) emphasized the need of better understanding of energy behavior of machining processes considering the time-dynamic nature of manufacturing processes. This section presents a structured algorithm to identify the operating status of a machine tool to quantify the energy consumption of a machine tool at the unit process level and determine the operational status of the machine tool using the energy data profile. It also identifies the activation of various components such as spindle motor, axis motors, coolant pump, automatic tool changer, etc. The proposed algorithm is a two-step non-intrusive approach to obtain the operational state and energy consumption of the machining system. In the first step, the system was trained using a series of algorithms including principal component analysis (PCA), k-nearest neighbor classifier (k-nn) and median absolute deviation (MAD) to identify and categorize the various machining states. In the second step, the algorithm was tested for a new set of data and the results were discretized. This algorithm works as a smart energy sensor which is trained to process the new data based on the prior information provided to it. It is a non-intrusive load monitoring approach and requires only the power data from the main supply of a machine tool. Hence, it reduces the complexity and high cost involved with multi-sensor arrangements. Matlab 2015 software was used to develop the proposed algorithm. The proposed algorithm can quantify the exact time duration and energy consumption for the three machining states – (i) Start-up state, (ii) Machine ready state and (iii) Cutting state. The methodology adopted for the present study is shown in Figure 3.11. The time

and energy map provided by the proposed sensor can help the practitioners to identify the potential areas of energy and time savings.

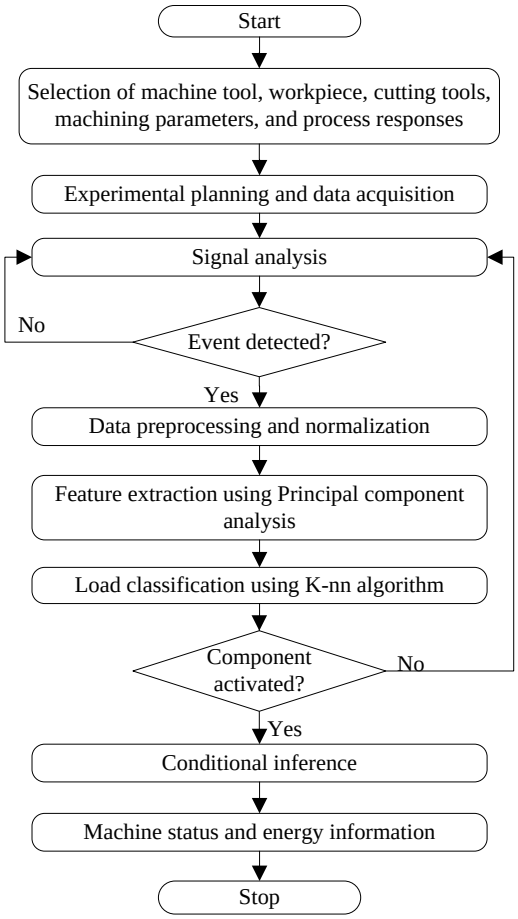

Figure 3.11 Methodology adopted for the development of the proposed structured algorithm

3.4.1 Algorithm Training

In the first step of methodology, the system was trained using a set of training data and data signature for each event was stored in the system library. Experiments were conducted to obtain the data required for training purpose including spindle rotation at eight different speeds ranging from 1000 RPM to 8000 RPM, activation of coolant pump, rotation of automatic tool changer and tool change. Each component was activated five times and the power signature was recorded at the main power supply. The power data was recorded in the form of a two dimensional matrix of power and time. Figure 3.12 shows the power profile obtained for spindle rotation at 6000 RPM.

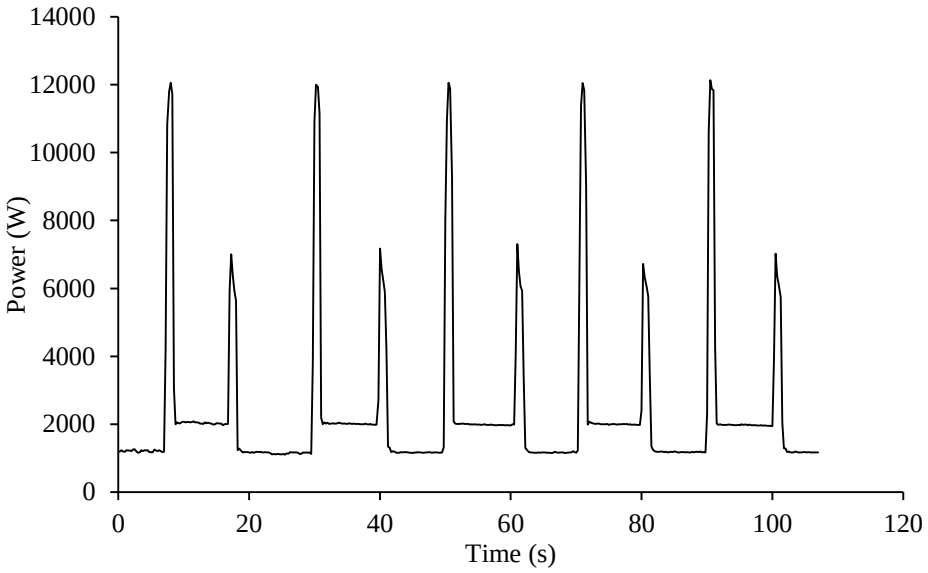

Figure 3.12 Power profile for spindle activation at 6000 RPM

The power profile for activation period was trimmed and normalized by subtracting the minimum power value from the RMS power waveform. Seven features were obtained for each activation load signature, which were unique for each event and used to assign a class label to an individual event. The seven features used in the present study are shown in Table 3.13.

Table 3.13 Details of the features extracted for power signature

Feature	**Computation**
RMS power	E_k
Minimum power (E_{min})	Min(E_k)
Maximum of normalized data ($Enorm_{max}$)	Max(E_k)-Min(E_k)
RMS of normalized data ($Enorm_{rms}$)	$\sqrt{\frac{1}{n}\sum(\mathrm{E}_k - \mathrm{E}_{min})^2}$
Mean of normalized data ($Enorm_{avg}$)	$\frac{1}{n}\sqrt{\sum(\mathrm{E}_k - \mathrm{E}_{min})}$
Standard deviation of normalized data ($Enorm_{SD}$)	$\sqrt{\frac{1}{n}\sum\left((\mathrm{E}_k - \mathrm{E}_{min}) - \mathrm{E}_{mean}\right)^2}$
Crest factor ($Enorm_{CF}$)	$Enorm_{max}/Enorm_{rms}$
Form factor ($Enorm_{FF}$)	$Enorm_{rms}/Enorm_{avg}$

The extracted features for each event were stored in a seven-dimensional data set in the system library. However, working with seven features was a tedious task and therefore the dimensions of the data were reduced using principal component analysis. Principal component analysis is a statistical procedure that uses an orthogonal transformation to convert a set of observations of possibly correlated variables into a set of values of linearly uncorrelated variables called principal components.

In the present study, based on scree plot two principal components were found to be adequate for analysis. The same procedure was used to obtain the two-dimensional data signature for each event. The data was stored in the system library for further requirement by the classification algorithm. The k-nn classifier was used to classify the events in various classes. The Euclidean distance between the test point and training data points stored in the system was calculated to assign a class to the test data point. The weight of each nearest neighbor was calculated as the inverse of the distance between the test point and the nearest neighbor.

3.4.2 Event Classification and Conditional Inference

Once the algorithm was trained, the system could detect and classify any new data signature. An event detection algorithm was used to identify the occurrence of an event. An event is detected when the slope of power profile increases by more than a predefined threshold m_1. The detection algorithm records the data until certain conditions are satisfied. The first condition is that the slope must fall down below a predefined threshold m_2 and second, adjacent RMS power values must satisfy certain conditions. The feature values m_1 and m_2 were selected based on the training data for the algorithm. In the training phase, power waveform was recorded for activation of various components. Each component was activated five times and the rise in slope for each activation was calculated. The mean of

five slope values was calculated to define feature values m_1 and m_2. After detection of an event, it was classified using k-nearest neighbor classification algorithm.

When the spindle was activated and the machine was ready for cutting, the system tried to identify the commencement of the cutting process. It looks for a significant rise in power using a median absolute deviation (MAD) algorithm. The system reads a number of power values at a time to calculate the median at every stage and compares it with the previous value. This helps to detect change in the energy consumption by the machine tool. Cutting starts when the value of median is higher than a predefined threshold. Hence, the algorithm detected the material removal process and calculated the processing time and energy consumption for cutting and no-cutting stages.

3.4.3 Case Study

In the present study, the proposed algorithm was tested for milling process on LMW klein KODI 40 VMC. A cuboidal aluminum block of size 70×70×50 mm was used as workpiece. The machining operations were selected based on the guidance provided by Japanese Standards Association on the design of standard workpiece (Behrendt et al., 2012). Five distinguishable features were machined on the workpiece including face milling, drilling, unidirectional slot, grooving, and bidirectional slot. The details of the workpiece features, processing sequence and corresponding machining parameters are as follows:

Operation 1: Face milling to remove a 3 mm layer from surface using 25 mm face mill

Operation 2: Drilling a diameter hole (Φ7mm x 30mm depth) using 7 mm drill

Operation 3: Machining a slot of 5 mm depth and 8mm width using 6 mm end mill

Operation 4: Machining a slot of 12 mm depth and 8mm width using 6 mm end mill

Operation 5: Machining a slot of 8 mm depth and 10 mm width using 8 mm end mill

The details of workpiece and machining parameters used in the study are shown in Figure 3.13 and Table 3.14, respectively.

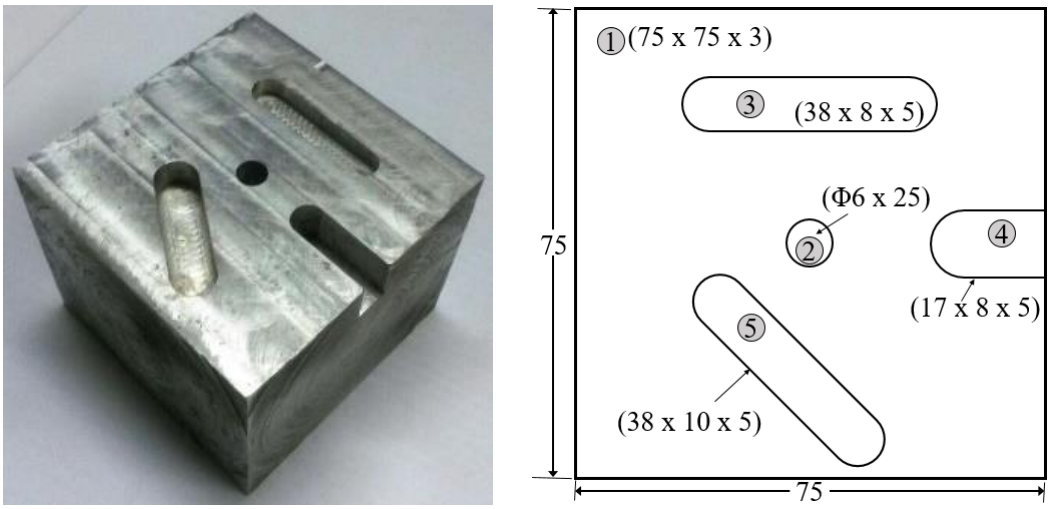

(all dimensions are in mm)

Figure 3.13 Details of the workpiece specimen

Table 3.14 Process parameters used in the case study

Operation number	1	2	3	4	5
Total Depth of operation (mm)	3	30	5	12	8
Feed rate X(mm/min)	50	50	50	50	50
Feed rate Y(mm/min)	-	-	-	-	50
Feed rate Z(mm/min)	100	100	100	100	100
Spindle speed (RPM)	6000	5000	6000	4000	5000
Coolant Pump	On	Off	On	On	On

The power profile for the machining process was recorded at the main power supply of the machine. Fluke 435 series ii three-phase power quality and energy analyzer was used to record the power. The detection and classification of spindle activation at 6000 RPM is shown in Figure 3.14(a-c) for brevity. The activation was detected when the slope of power waveform increased beyond a predefined threshold. The recorded spindle activation data was normalized and seven features were extracted as described in section 3.4.1.The data was then transformed and plotted in a two-dimensional space. Figure 3.14 shows various data points plotted in two-dimensional space and the highlighted point

shows the spindle activation detection. The inverse Euclidean distance between the highlighted point and each of the other points was calculated using k-nn algorithm for classification of the data point and it was assigned the class 'RPM6000'. Similarly, the activation of coolant pump was identified and classified. Once spindle and coolant pump were activated and the system was stabilized, it started to search for a hike in power data and hence identified commencement of the cutting process. The system continued to record the power data for the cutting process until power dropped below a threshold value and cutting was stopped. Figure 3.15 shows the power profile obtained for the five cutting operations performed in the present study.

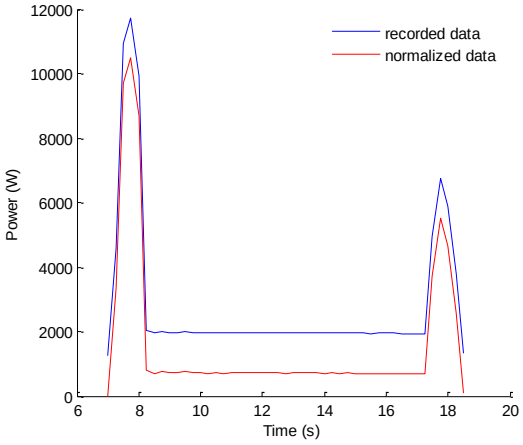

(a)

Feature	Value
$Enorm_{max}$	10.760 kW
$Enorm_{rms}$	3.334 kW
$Enorm_{avg}$	1.910 kW
$Enorm_{std}$	3.026 kW
$Enorm_{time}$	13 sec
$Enorm_{CF}$	3
$Enorm_{FF}$	2
Class label	RPM6000

(b)

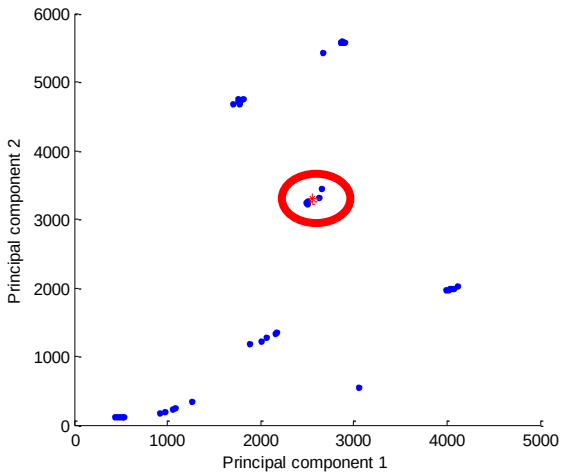

(c)

Figure 3.14 Identification, power signature and classification of spindle activation at 6000 RPM

The proposed algorithm followed the same approach for the remaining power profile and identified five spindle activations, three tool changes, and five coolant pump activations. The algorithm identified the cutting and no-cutting states of the machine and successfully quantified the cutting duration for each operation. The red points show the cutting zone and green points show the non-cutting zone in Figure 3.15. The energy consumed in each machining state was also quantified successfully. The summary of results provided by the algorithm is shown in Figure 3.16.

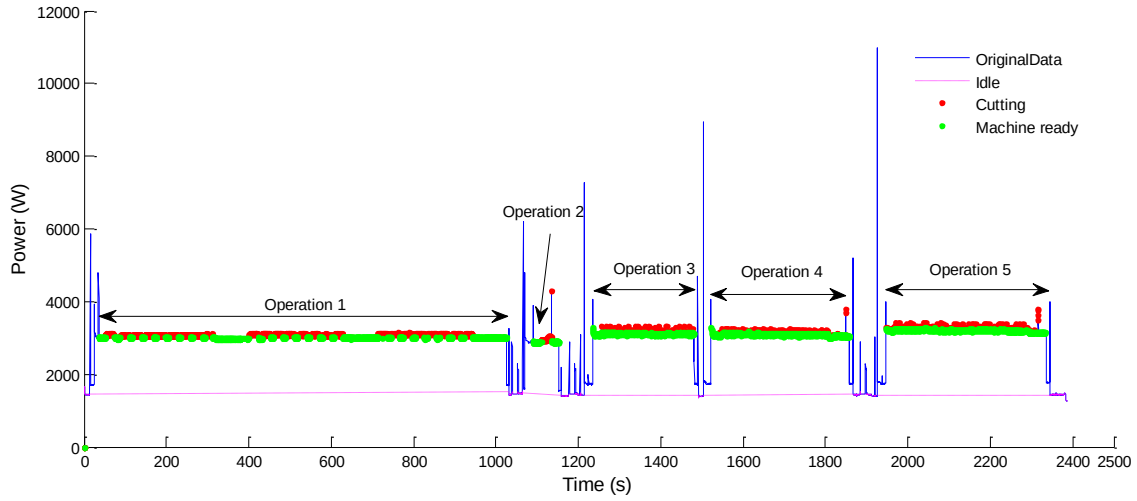

Figure 3.15 Identification of cutting and no-cutting zones using the proposed algorithm

****
Time spent in stand-by state: 8.15%
Time spent in machine ready state: 48.18%
Time spent in cutting state: 43.7%
Energy consumption in stand-by state: 4.04%
Energy consumption in machine ready state: 48.69%
Energy consumption in cutting state: 47.3%
****

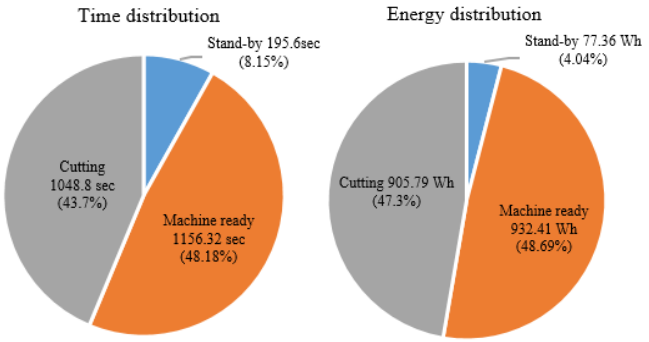

Figure 3.16 Time and energy consumed for each machining state for the test workpiece

It is evident from Figure 3.16 that the cutting operation consumed only 43.7% of total processing time whereas machine ready state consumed 48.18% and stand-by state consumed 8.15% of the total processing time. In the total energy consumption, the share of cutting operation was 47.3%, whereas the shares of machine ready state and stand-by state were 48.69% and 4.04%, respectively. The results of the algorithm can be used as a basis for identification of potential saving areas to improve energy performance of the machine tools.

3.5 MODELLING OF CARBON EMISSIONS

The carbon emissions refer to the amount of CO_2 generated during a machining process. It is measured in terms of $kgCO_2$ equivalent. In a machining process, the carbon emissions are caused due to various factors such as energy consumption by the machine tool, production and transportation of the raw material, consumption of cutting tools, production and disposal of used coolant, metal chip post-processing, etc. The carbon emissions during machining process are modelled as the summation of carbon emissions caused by these factors.

$$CE_{process} = CE_{energy} + CE_{coolant} + CE_{cutting\ tool} + CE_{material} + CE_{chips} \quad (3.23)$$

The system boundary of the machining process under consideration is given in Figure 3.17.

3.5.1 Carbon Emissions due to Energy Consumption (CE_{energy})

CNC machine tools consume energy in the form of electricity. The carbon emissions caused due to electrical energy consumption can be modelled as follows (Li et al., 2015):

$$CE_{energy} = CEF_{energy} * EC_{process} \quad (3.24)$$

where CEF_{energy} is the carbon emission factor for electricity ($kgCO_2/kWh$) and $EC_{process}$ is the energy consumed during the machining process. The calculation for energy consumption for the machining process has been discussed in section 3.3.

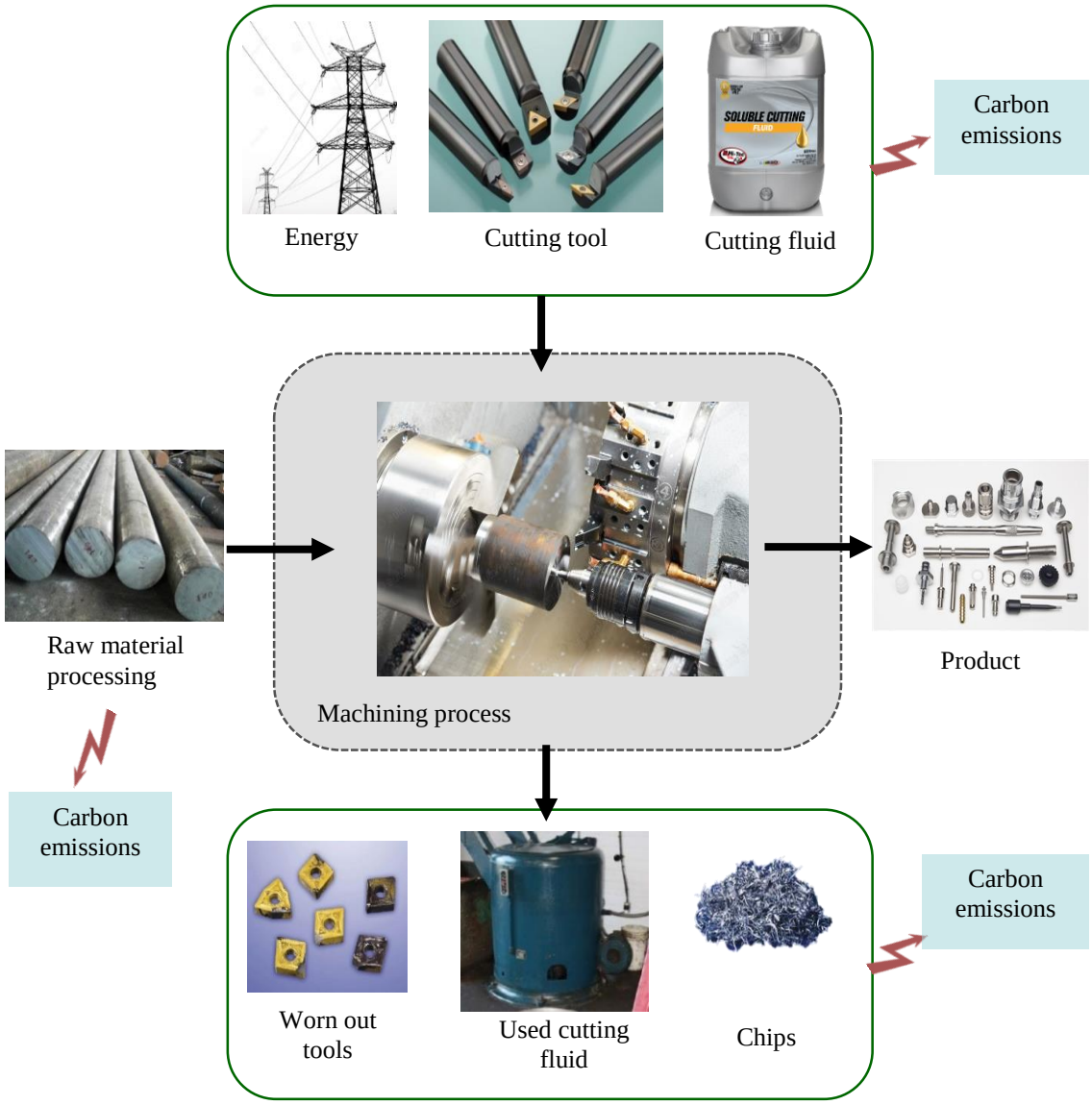

Figure 3.17 System boundary of the machining process

The production of electrical energy causes carbon emissions at the power plant, therefore, the CEF_{energy} varies considerably depending on the power plant location,

resources and technology used, and seasonal variations. The carbon intensity of some common fuels is obtained from literature and provided in Table 3.15.

Table 3.15 Carbon intensity of common energy sources (Gutowski, 2007)

Energy source	Carbon intensity (gC/MJ)
Coal (carbon)	30
Oil (0.856 g C/g Oil)	20
Gasoline (octane)	18.5
Natural gas (methane)	15

The carbon emissions generated due to electricity production for different countries differ significantly. Figure 3.18 shows the energy mix compositions for different countries. It is observed that the carbon emissions for the countries which depend mostly on the conventional thermal power plants (like Australia, Saudi Arabia, Poland, etc.) is higher as compared to carbon emissions for the countries which have switched to renewable energy sources (like Brazil, Norway, Canada, etc.). International Energy Agency published a report on the composite electricity/heat emission factors for different countries. However, these factors include the emissions from electricity as well as heat generation and therefore do not accurately represent the grid electricity emissions. The emissions due to heat generation may bias the emission factors. Brander et al. (2011) conducted a study to calculate the electricity specific emission factors for different countries based on alternative data published by IEA about the total emissions caused by electricity generation and total electricity produced by each country. The carbon emissions factor due to electricity production for different countries is also provided in Ecoinvent dataset, commonly used for life cycle assessment studies. The carbon emission factors for energy generation for different countries provided by different sources are given in Table 3.16.

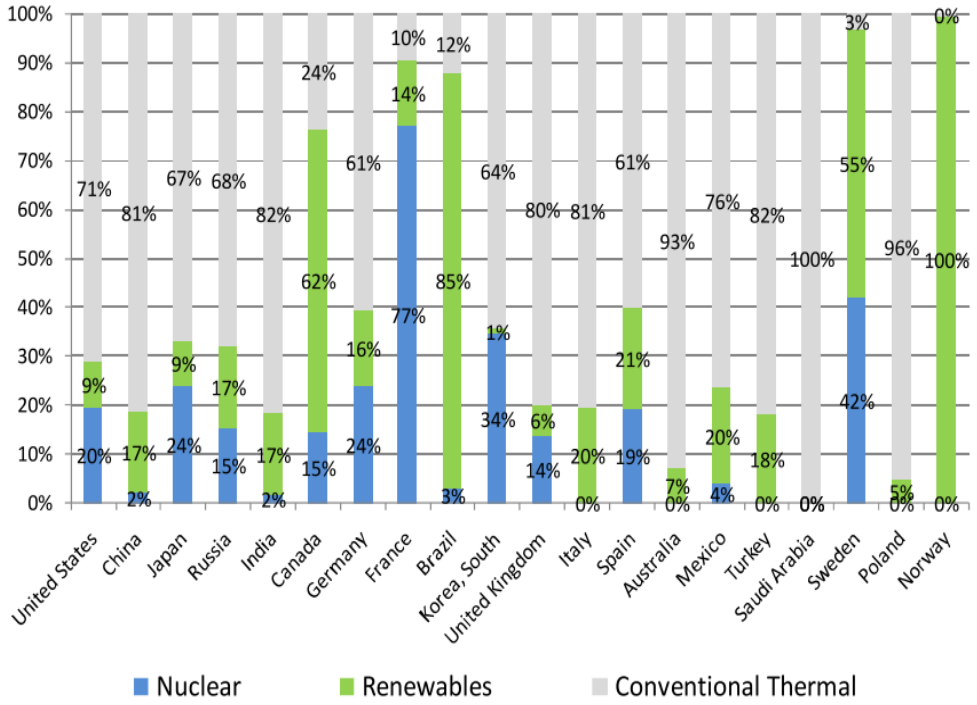

Figure 3.18 Type of electricity generation for different countries (Herrmann et al., 2010)

Table 3.16 Carbon emission factors for electricity generation for different countries by different sources

S.No.	Country	CEF ($kgCO_2/kWh$)		
		(Ecoinvent 3.0)	(Brander et al., 2011)	(IEA)
1	USA	0.41	0.5471	0.5350
2	China	1.14	0.9746	0.7448
3	Japan	0.63	0.4435	0.4364
4	Russia	0.71	0.5132	0.3255
5	India	1.41	1.3331	0.9682
6	Canada	0.12	0.1797	0.1805
7	Germany	0.65	0.6722	0.4411
8	France	0.11	0.0709	0.0827
9	Brazil	0.26	0.0926	0.0888
10	South Korea	0.62	0.4946	0.4813
11	United Kingdom	0.66	0.5085	0.4869
12	Italy	0.61	0.4108	0.3984
13	Spain	0.48	0.3429	0.3258
14	Australia	1.12	0.9917	0.8833
15	Mexico	0.67	0.4525	0.4399
16	Turkey	0.66	0.8656	0.4952
17	Saudi Arabia	0.85	0.7956	0.7541
18	Sweden	0.06	0.0230	0.0399
19	Poland	1.10	1.1961	0.6534
20	Norway	0.02	0.0022	0.0052

3.5.2 Carbon Emissions due to Cutting Tool (CE_{tool})

Cutter tool wear during machining is inevitable. The embodied energy of the cutting tool is consumed as indirect energy during the machining process. The carbon emissions caused due to production, disposal, and recovery process of cutting tools can be calculated as follows (Narita and Fujimoto, 2009):

$$CE_{tool} = \frac{t_{cutting}}{\sum_{j=1}^{Nr} T_{tool,j}} * \left[\left(CEF_{tool} + CEF_{tool,dis}\right) * W_{tool} + N * CEF_r\right] \quad (3.25)$$

where CEF_{tool} is the carbon emission factor for the production of cutting tool ($kgCO_2/kg$), $CEF_{tool,dis}$ is the carbon emission factor for the disposal of cutting tool ($kgCO_2/kg$), W_{tool} is the weight of the cutting tool, $T_{tool,j}$ is the tool life at each recovery, N is the number of recoveries by re-sharpening the tool, and CEF_r is the carbon emission factor for the recovery of cutting tool ($kgCO_2/kg$).

It is observed that the carbon emissions caused due to disposal and recovery of the cutting tools are very less as compared to the carbon emissions caused due to the production of the cutting tools. Therefore the carbon emissions caused due to disposal and recovery of the cutting tools are neglected. The simplified equation for carbon emissions caused due to use of the cutting tools is given as follows (Li et al., 2015):

$$CE_{tool} = CEF_{tool} * W_{tool} * \frac{t_{cutting}}{T_{tool}} \quad (3.26)$$

where T_{tool} is the total tool life. Generally, a cutting tool is re-sharpened N times before changing the tool. Hence, total tool life (T_{tool}) is calculated as (N+1)T, where T refers to the tool life. The cutting tool can be used for material removal until the tool wear is within the permissible limits. When the tool wear condition reaches the tool wear criterion, the tool is either re-sharpened or regarded as a scrap. Tool life depends on several factors such

as the cutting parameters, coolant conditions, workpiece properties, etc. The tool life can be calculated using extended Taylor's equation, as follows:

$$T = \frac{1000\, z\, C_{tool}}{\pi^m D^m n^m f^r a_p^k} \tag{3.27}$$

where C_{tool} is the tool life coefficient, z is the number of cutting edges and m, r, k are the indices for cutting speed, feed and depth of cut, respectively.

CEF_{tool} can be calculated based on the energy footprint of the cutting tool (E_{tool}) and weight of the cutting tool.

$$CEF_{tool} = \frac{CEF_{energy} * E_{tool}}{W_{tool}} \tag{3.28}$$

Rajemi et al. (2010) investigated the energy footprint for the cutting tools considering two cases. In the first case, the embodied energy of cutting tool material and energy required for tool manufacturing were considered to calculate the energy footprint of the cutting tool, whereas in the second case only the energy required for tool manufacturing was considered. The energy footprint for a cutting tool weighing 9.5g and manufactured by sintering process was estimated to be 5.3 MJ and 1.5 MJ for cases 1 and 2, respectively.

3.5.3 Carbon Emissions due to Coolant ($CE_{coolant}$)

The production, use and disposal of coolant also cause carbon emissions. Generally, two types of cutting fluids are used in machining activities: water-soluble and water-insoluble cutting fluids.

Water-soluble cutting fluid is a mixture of water and mineral oil. During the machining process, some of the cutting fluid is lost due to evaporation, adsorption by the chips, leakage, etc. Therefore, extra coolant is added to maintain the required concentration and volume of the cutting fluid. The calculation of cutting fluid consumption based on the flow

rate is difficult due to additional supply and recycling of the cutting fluid. Therefore, the carbon emissions are calculated based on the replacement period of the cutting fluid. $CE_{coolant}$ for water soluble cutting fluid is calculated as follows:

$$CE_{coolant} = \frac{PT}{T_{coolant}} * \left[CEF_{coolant} * (V_{in} + V_{ad}) + CEF_{coolant-dis} * \frac{(V_{in}+V_{ad})}{\delta}\right] \quad (3.29)$$

where $T_{coolant}$ is the average interval of coolant change, PT is the processing time, $CEF_{coolant}$ and $CEF_{coolant-dis}$ are the carbon emission factors for production and disposal of coolant respectively ($kgCO_2$/kg of the cutting fluid), V_{in} is the volume of cutting fluid used initially, V_{ad} is the volume of additional cutting fluid used before coolant replacement, and δ is the concentration of the coolant. Since, the carbon emissions caused by water usage is negligible as compared to soluble oil, it is not considered in the present study.

For water-insoluble cutting fluids, the carbon emissions are calculated based on the cutting fluid discharge rate as follows (Narita and Fujimoto, 2009):

$$CE_{coolant} = \frac{PT}{3600} * \frac{\dot{V}}{1000} * (CEF_{coolant} + CEF_{coolant-dis}) \quad (3.30)$$

where $\dot{V}$ is the discharge rate of the cutting fluid (cc/h). $CEF_{coolant}$ is computed based on the embodied energy and the carbon intensity of the coolant oil.

$$CEF_{coolant} = EE_{coolant} * CI_{coolant} * \frac{44}{12} \quad (3.31)$$

where $EE_{coolant}$ is the embodied energy of the coolant oil (GJ/L) and $CI_{coolant}$ is the carbon intensity of the coolant oil (kgC/GJ).

The embodied energy of the mineral oil ranges from 41,868 to 42,705 kJ/kg. The carbon intensity of the mineral oil is 20 kgC/GJ (IPCC, 2008). The density of mineral oil at normal temperature and pressure conditions lies between 0.86-0.98 g/cm^3.

$CEF_{coolant-dis}$ can be considered to be same as the carbon emission factor for waste water disposal due to low concentration of coolant oil in water based cutting fluid. IPCC (2008) reported the carbon emission factor for waste water disposal as 0.2 $kgCO_2/L$.

3.5.4 Carbon Emissions due to Raw Material Production ($CE_{material}$)

During the machining operation, the raw material is converted into useful products by removing material in the form of small chips. The embodied energy of the removed material is indirectly consumed during the machining process and adds to the carbon emissions. The carbon emissions caused due to production of raw material can be calculated as follows:

$$CE_{material} = CEF_{material} * MRV * \rho \tag{3.32}$$

where $CEF_{material}$ is the carbon emission factor for production of raw material ($kgCO_2/kg$), MRV is the volume of removed material in the form of small chips and ρ is the density of the workpiece material (kg/mm^3). $CEF_{material}$ can be calculated as follows:

$$CEF_{material} = EE_{material} * CEF_{energy} \tag{3.33}$$

where $EE_{material}$ is the embodied energy of the raw material (MJ/kg) and CEF_{energy} is the carbon emission factor of the energy mix used for the production of raw material ($kgCO_2/MJ$). The embodied energy and carbon emission factors for aluminum are 191 MJ/kg and 16.13 $kgCO_2/kg$, respectively (Gutowski, 2007; Li et al., 2015).

3.5.5 Carbon Emissions due to Chip Processing (CE_{chips})

The chips produced by machining processes are cleaned and recycled. The chip recycling is generally an energy intensive process and leads to carbon emissions. The carbon emission caused due to processing of metal chips is calculated as

$$CE_{chips} = CEF_{chips} * MRV * \rho \quad (3.34)$$

where CEF_{chips} is the carbon emission factor for chips ($kgCO_2/kg$). CEF_{chips} depends on the material of the chips and technology used for recycling. CEF_{chips} can be calculated as the product of energy used for chip recycling and the carbon emission factor of the energy mix used for the chip recycling.

3.6 SUMMARY

In this chapter, the experimental models for the energy consumption by different machine tool components were provided. The energy models were used to develop a smart energy metering system based on non-intrusive load monitoring approach for low-cost data acquisition and analysis. The smart metering system was developed in the form of a structured algorithm using a series of feature-extraction and classification algorithms such as principal component analysis, k-nn, and median absolute deviation. It required energy measurement at main supply of the machine tool and split the individual loads to quantify time duration and energy consumption of each machining state. It integrated load monitoring with condition inference techniques to identify the operating status of a machine tool through the activation of various components. This algorithm eliminated the high cost and complexity involved with multi sensor systems. The proposed algorithm was validated for a vertical milling center. This algorithm has potential to be adapted for industry 4.0 applications. The potential energy saving area can be identified using the proposed algorithm. This will assist the practitioners in decision making for adopting more sustainable strategies. In the second part of the chapter, experimental models for carbon emissions caused by different factors – energy consumption, material processing, production and disposal of cutting fluids, cutting tool production, lubricant consumption, etc. – during the machining process were provided.